Nucl. Sci. and Tech, Vol.5, No. 3 (2015), pp. 19-31

Nuclear Science and Technology

Journal homepage: https://jnst.vn/index.php/nst

Multi codes and multi-scale analysis for void fraction prediction in hot channel for VVER-1000/V392

Hoang Minh Giang[1], Hoang Tan Hung[1], Nguyen Huu Tiep[2]

[1]Nuclear Safety Center, Institute for Nuclear Science and Technology

[2]Nuclear Power Center, Institute for Nuclear Science and Technology

Abstract: Recently, an approach of multi codes and multi-scale analysis is widely applied to study core thermal hydraulic behavior such as void fraction prediction. Better results are achieved by using multi codes or coupling codes such as PARCS and RELAP5. The advantage of multi-scale analysis is zooming of the interested part in the simulated domain for detail investigation. Therefore, in this study, the multi codes between MCNP5, RELAP5, CTF and also the multi-scale analysis based RELAP5 and CTF are applied to investigate void fraction in hot channel of VVER-1000/V392 reactor. Since VVER-1000/V392 reactor is a typical advanced reactor that can be considered as the base to develop later VVER-1200 reactor, then understanding core behavior in transient conditions is necessary in order to investigate VVER technology. It is shown that the item of near wall boiling, Γ_w in RELAP5 proposed by Lahey mechanistic method may not give enough accuracy of void fraction prediction as smaller scale code as CTF.

Keywords: *VVER, CTF, RELAP5, multi-scale, void fraction, hot channel…*

I. INTRODUCTION

A multi codes approach is an establishment initial and boundary conditions for a code from output of another. Coupling codes approach is interactive exchange data between codes such as PARCS and RELAP5 [1]. When this coupling is enabled, the 3-D reactor kinetics calculated by PARCS code affects to the heat structure modeling for heat source in RELAP5. Therefore, the heat source modeling is improved with better initial data and core power is calculated by PARCS instead of RELAP5. The multi-scale analysis [2] is considered as an approach to combine the advantage of increased computer power and improved simulation tools for water-cooled reactor thermal hydraulics analysis. This analysis approach is often illustrated with four scales corresponding to four kinds of simulation software, as shown in Figure 1. These scales are the system, component, meso-scale (also referred as CFD), and the micro scale (also referred as DNS scale).

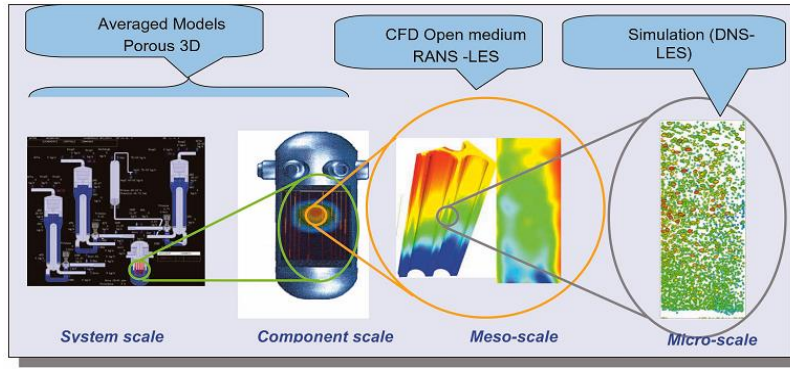

Fig.1. Illustration of the Multi-Scale Analysis for Reactor Thermal hydraulics [2]

https://doi.org/10.53747/jnst.v5i3.196
(Received 17 July 2015, accepted 17 September 2015)

As illustrated in Figure 1, it is possible to conceive that a system code can predict the behavior of the primary circuit and gives boundary conditions to a component code for the core thermal hydraulics. Within the core, a few sub-channels could be simulated with a CFD for open medium, using the component code results as boundary conditions. By switching analysis to a finer scale, a specific part of the domain can be simulated with phenomena occurring in smaller scale. Therefore, it could be aware of more accuracy given by finer scale simulation tool in comparison with experiment data. Thus, in this study, the approach of multi codes, which are MCNP5, RELAP5 and CTF, is applied to investigate void fraction in hot channel of VVER-1000/V392 reactor. The results calculated independently by MCNP5 code give the axial power distribution and radial peaking factor in order to simulate heat structure and hot channel power in RELAP5 and also give the power distribution for each fuel rod in the hot channel. Then, the multi scale analysis is conducted by RELAP5 and CTF as system scale and component scale. The results from system scale analysis are transferred to CTF, a version of COBRA-TF, which is finer scale analysis tool. It is expected that the final results of void fraction prediction is more accuracy by this approach of multi codes and multi scale analysis. Even a lot of studies related to VVER-1000 reactors such as Kozloduy [3], Kudankulam [4], are presented, this study uses data from Belene project which is also first study on VVER-1000/V392 in Vietnam.

II. PHYSICAL MODELS FOR VAPOR GENERATION AND CONDENSATION

A. Brief of vapor generation and condensation in RELAP5

The vapor generation or condensation [5] in RELAP5 is modeled by phase change induced from heat transfer between interface and wall heat transfer effect:

$$\Gamma_g = -\frac{H_{ig}(T^s - T_g) + H_{if}(T^s - T_f)}{\left(h_g^* - h_f^*\right)} + \Gamma_w \quad (1)$$

Where:

$\left(h_g^*, h_f^*\right)is\left(h_g^s, h_f\right)$ or $\left(h_g, h_f^s\right)$ in case of vaporization or condensation, respectively.

$$\Gamma_f = -\Gamma_g \quad (2)$$

The item , Γ_w, denotes interfacial vaporization or condensation rate in the boundary layer near the wall as described by (3) or (4), respectively.

$$\Gamma_w = -\frac{Q_{if}^w}{\left(h_g' - h_f'\right)} \quad (3)$$

$$\Gamma_w = -\frac{Q_{ig}^w}{\left(h_g' - h_f'\right)} \quad (4)$$

The item,(h_g', h_f'), is chosen similar to $\left(h_g^*, h_f^*\right)$ but it denotes for phasic enthalpies associated with wall (thermal boundary layer).

B. Brief of CTF models for evaporation and condensation

Evaporation and condensation induced by thermal phase change

The CTF model includes nine conservation equations and three fields: liquid, vapor and entrained liquid drop. The various forms of conservation equations are presented [4, 5]. There are two different types of flow regime maps: “normal wall” map and “hot wall” map. The normal wall map is used when the maximum wall surface temperature, T_w, in a given computational mesh cell is below the critical heat flux temperature, T_{crit}. Then a part of wall adjacent to this mesh cell is expected to be fully wetted. The normal wall flow regime map includes the following flow regimes: small bubble; small-to-large bubble (slug); churn/turbulent; and annular/mist.

In the sub cooled region, heat transfer from the wall partitioned only into liquid is given by:

$$q_w''' = h_c(T_w - T_l)\frac{A_s}{A_x \Delta X} \quad (5)$$

Whenever heat from the wall is transferred to liquid, liquid enthalpy increases and the phase change which is expressed via volumetric mass flow rate, Γ''', is provided by:

$$\Gamma''' = \left[\frac{A'''_{int,shl} h_{i,shl}}{(h_{g,sat} - h_{l,sat}) C_{pl}} \left|h_l - h_{l,sat}\right| + \frac{A'''_{int,shv} h_{i,shv}}{(h_{g,sat} - h_{l,sat}) C_{pv}} \left|h_g - h_{g,sat}\right|\right] - \left[\frac{A'''_{int,scl} h_{i,scl}}{(h_{g,sat} - h_{l,sat}) C_{pl}} \left|h_l - h_{l,sat}\right| + \frac{A'''_{int,scv} h_{i,scv}}{(h_{g,sat} - h_{l,sat}) C_{pv}} \left|h_g - h_{g,sat}\right|\right] \quad (6)$$

Evaporation and condensation induced by turbulent mixing and void drift

Another phenomenon that causes phase change is turbulence. The CTF's turbulent mixing and void drift uses a simple turbulent-diffusion model by calculating the lateral velocity from sub channel to sub channel. Based on the turbulent mixing model, the mass exchange of phase (k), $\dot{m}_k^{TM}$ induced by subchannel (i) and (j) is defined as:

$$\dot{m}_k^{TM} = \beta_{TP} \frac{\bar{G}}{\bar{\rho}} \left(\alpha_{kj}\rho_{kj} - \alpha_{ki}\rho_{ki}\right) \quad (7)$$

The mass exchange, $\dot{m}_k^{VD}$ due to drift model is obtained:

$$\dot{m}_k^{VD} = \beta_{TP} \frac{\bar{G}}{\bar{\rho}} \left(\alpha_{kjEQ}\rho_{kjEQ} - \alpha_{kiEQ}\rho_{kiEQ}\right) S_k \Delta X \quad (8)$$

The item β_{TP} is Beus's correlation for two-phase turbulent mixing coefficient [9].

C. Brief information of VVER-1000/V392

The main parameters for the VVER-100/V392 reactor with adaptation in Belene project (called VVER-1000/V466) are given in Table I.

Table I. Primary circuit technical characteristics of VVER-1000/V392 reactor [8]

Characteristic	Value
Nominal thermal power of the reactor, MWth	3000
Number of circulation loops	4
Coolant pressure at the reactor outlet (absolute), MPa	15,7+0,3
Coolant temperature at the reactor inlet, °C	291
Coolant temperature at the reactor outlet, °C	321
Coolant flow through the reactor, m^3/h	86000
Fuel height in the core in cold state, m	3.53
Number of fuel assemblies in the core, pcs.	163
Pitch between FAs, mm	236

III. RESULTS AND DISCUSSIONS

A. Power distributions calculations by MCNP5

The arrangement of 163 fuel assemblies in the core is presented in Figure 2. Since the symmetry of the loading pattern of the first cycle (fresh fuel), the left graph of Figure 2 gives an illustration for 1/6 of the core including several types of fuel assemblies such as 22A, 30A9P, 39A6P and 39A9P. More detail about loading pattern for each fuel cycle and enrichment of each type of fuel assembly is presented in [9].

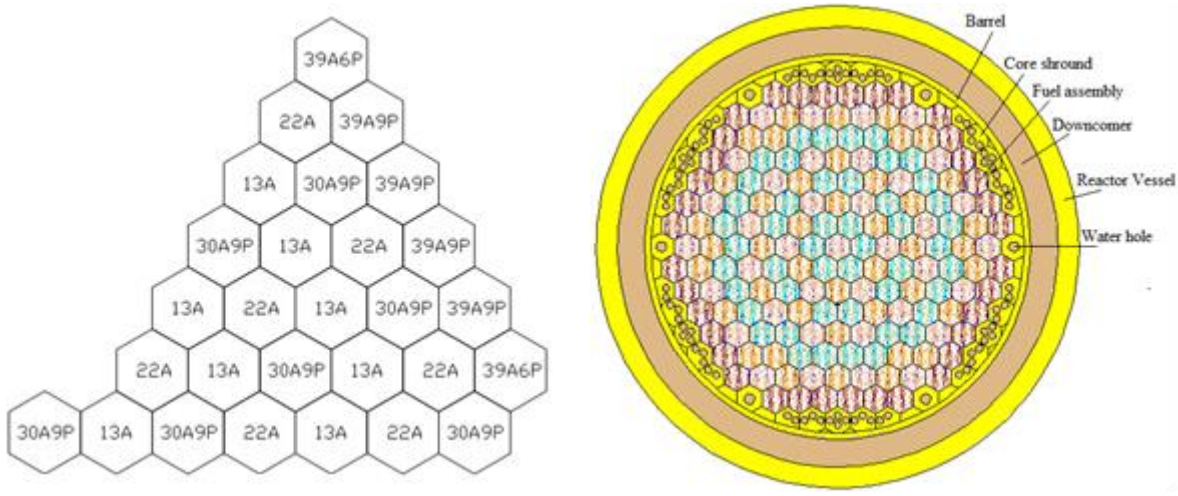

Fig. 2. The sixth of core loading pattern and whole core geometry for MCNP5 simulation

With regard to verification MCNP5 modeling in this study, the benchmark problem [16] was investigated in order to compare results from this study with other publications. It is shown that the results of average fission rate distribution calculation for state 1 to state 6 are different with those in benchmark publications about 4-5%. Therefore, it confirmed the appropriate MCNP5 modeling for reactor of VVER-1000/V392.

The calculation results are based on whole core geometry simulation and the number of neutron historiesequal 2.10^7 (with relative variation for k_{eff} around 10^{-5}). The relative power for each assembly in 1/6 of the core is presented in Figure 3. Thus, the hot channel is an assembly with identification of 30A9P corresponding tomaximum relative factor of 1.72. This value of power distribution is appropriate because it is within the range of (1.6, 1.8) mentioned in Safety Analysis Report [9].

For the RELAP5 heat structure modeling, it is always assumed that the axial power distribution for average channel and hot channel is the same, so MCNP5 is applied to calculate this distribution based on the assembly that is taken as the hot channel. As mention above, the calculation model for calculation of power distribution is validated through the benchmark problem, so that the pin-by-pin power distribution and power distribution along axial in the hottest fuel assembly is also accepted. Figure 4 shows the axial channel distribution of relative power with the maximum peaking factor of 1.52 that is also appropriate with distribution for the first fuel cycle as mentioned in [9].

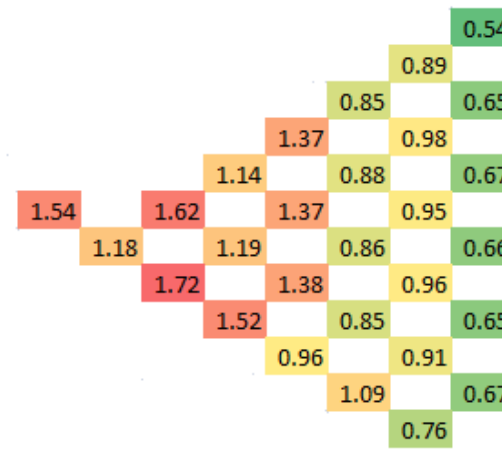

Fig. 3. The relative power distribution in the sixth of the whole core

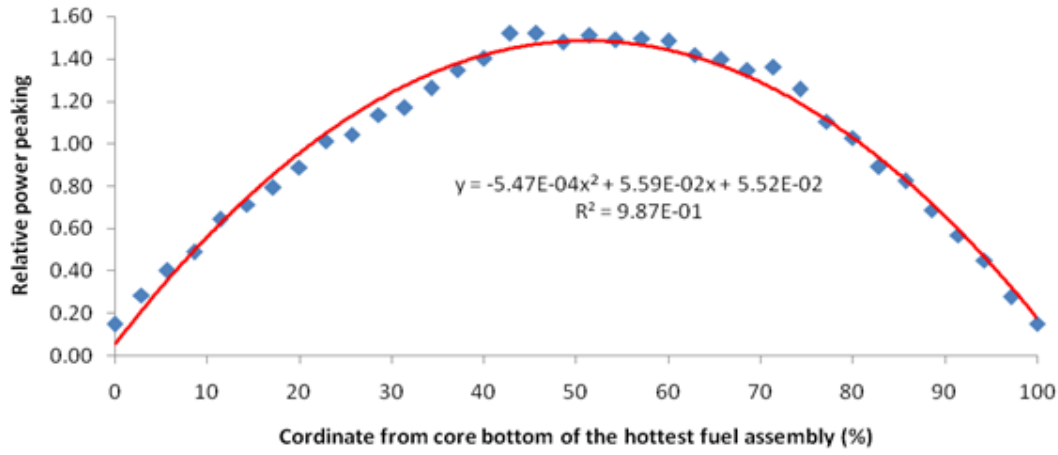

Fig. 4. Distribution of relative power along axial hot channel

For the CTF heat flux modeling, it is also needed the distribution of power inside each rod of hot channel and this calculation results are also performed by MCNP5. As mention above, our results of power distribution were confirmed, so it can be said that the result of pin-by-pin power distribution and power distribution along axial in the hottest fuel assembly was trusted. Figure 5 shows the relative power distribution for each rod inside the hot channel with maximum peaking factor of 1.374.

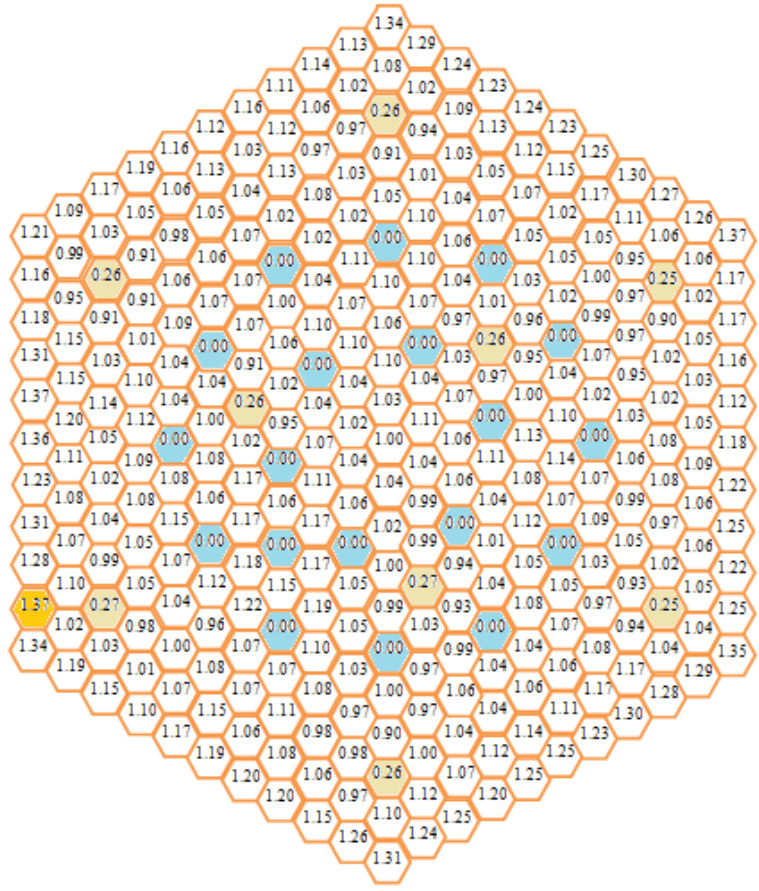

Fig.5. Distribution of relative power in the hot channel

B. System code RELAP5 analysis for void fraction prediction

The RELAP5 simulation for VVER-1000/V392 reactor is presented in [10] where the steady state calculation is compared with several main parameters of the design and the Safety Analysis Report [13] with good agreement. In this study, the power distribution along axial average and hot channel is taken from MCNP5 calculation results as illustrated in Figure 4.

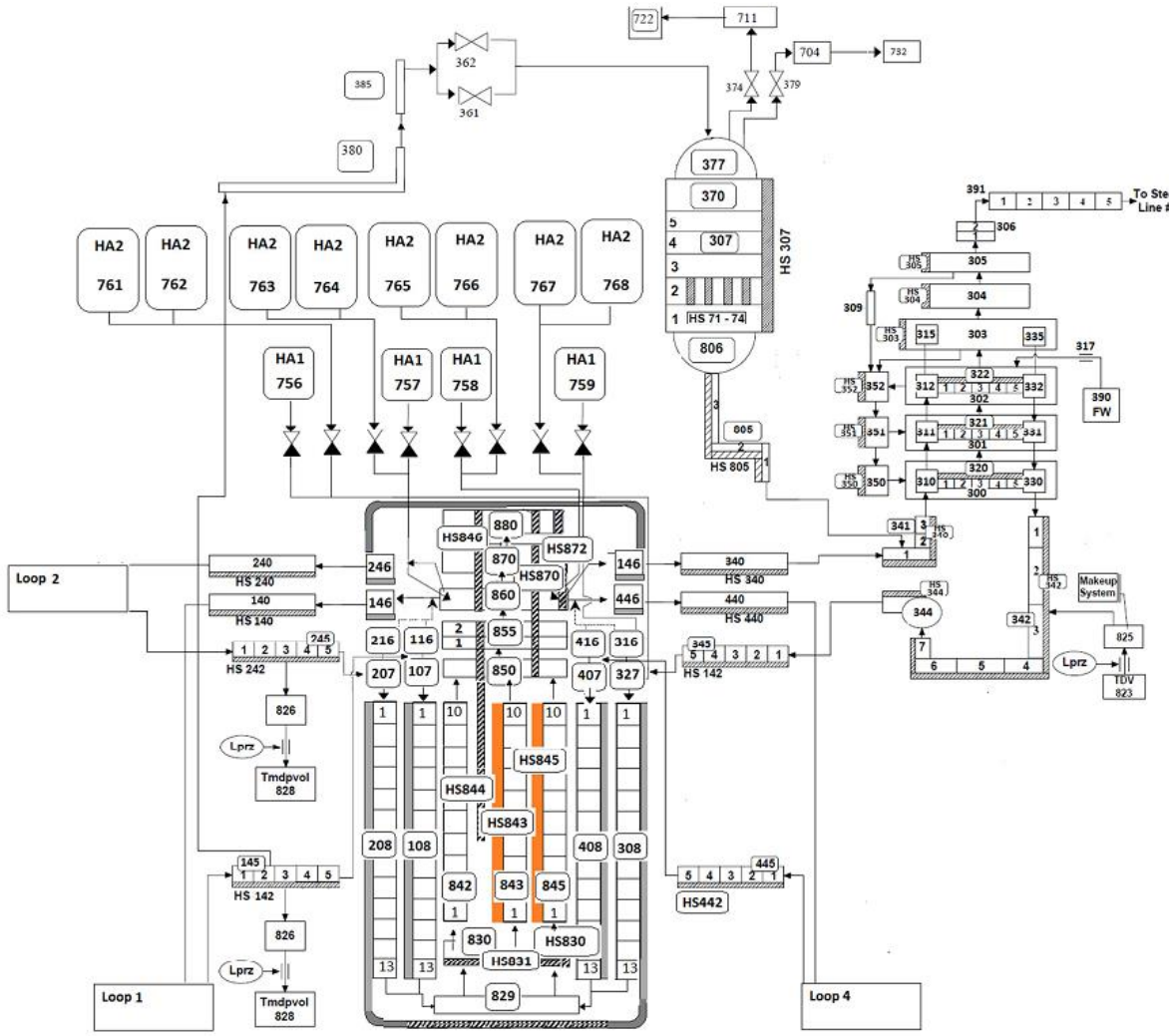

Fig. 6. Nodalization scheme for VVER-1000/V392 reactor [10]

Figure 6 shows the nodalization scheme used in this study. The average channel consist of 162 fuel assemblies and the hot channel is determined by the fuel assembly (30A9P) with relative power factor calculated by MCNP5 with the value of 1.72

In order to investigate void fraction prediction due to phase change, a spectrum of LOCAs and SBO simultaneous occurrences is studied with transient time to 40 seconds. Table 2 gives case studies and Table 3 gives the boundary conditions for LOCAS coupled with SBO analysis. Figure 7 shows the whole fuel assembly simulated as the hot channel and the active part on exit hot channel with the length of 0.44125m. The average value of void fraction prediction for this part is calculated by RELAP5 at system scale.

Table II. Case studies for void fraction prediction

Case ID	Description	Break Area (m^2)	Equivalent Diameter (m)	Location of break
LB01001	Large break LOCA coupled with SBO-1	0.11	0.374	Cold Leg
LB01002	Large break LOCA coupled with SBO-2	0.095	0.348	Cold Leg
SB01003	Small break LOCA coupled with SBO-1	0.07	0.298	Cold Leg
SB01004	Small break LOCA coupled with SBO-2	0.05	0.252	Cold Leg

Table III. Boundary condition of LOCA coupled with SBO for analysis

System	Event 3 (SAR)	Event 3 (The present study)
Scram signal	Actuated as a result of the LOOP	Actuated as a result of the LOOP
PRZ heaters	Not Operable because of the LOOP	Not Operable because of the LOOP
Primary make-up system	Not Operable because of the LOOP	Not Operable because of the LOOP
HA-1	All are available	All are available
HA-2	All are available	All are available
High Pressure Injection System (HPIS)	Trains 3 and 4 are available	Trains 3 and 4 are available
Low Pressure Injection System (LPIS)	Trains 3 and 4 are available	Trains 3 and 4 are available
Loss of Offsite Power (LOOP)	In the moment of accident initiation	In the moment of accident initiation
Diesel Generator (DG)	DG1 in repair, DG3 is failed	DG1 in repair , DG3 is failed
SG Active Heat Removal System (SAR SG)	SAR SG2 and 4 are available	SAR SG2 and 4 are available
SG PHRS	SG1 and 2 PHRS are operate	SG1 and 2 PHRS are operate

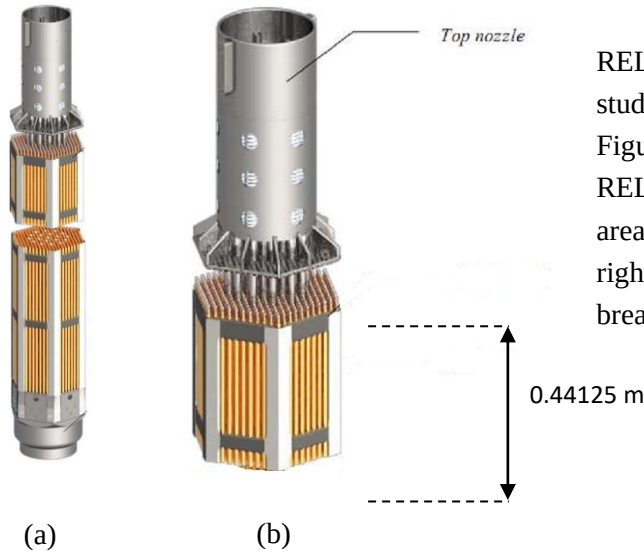

Fig. 7. (a) Whole fuel assembly [12] simulated as hot channel and (b) the active part for prediction of average void fraction at system scale

The calculation results given by RELAP5 are presented in Figure 8 for cases study as mentioned in Table 2.The left graph of Figure 8 shows the void fraction calculated by RELAP5 for two cases of LBLOCAs with beak area larger than $1ft^2$ (0.09290304 m^2) and the right graph shows two cases of SBLOCAs with break area less than $1ft^2$.

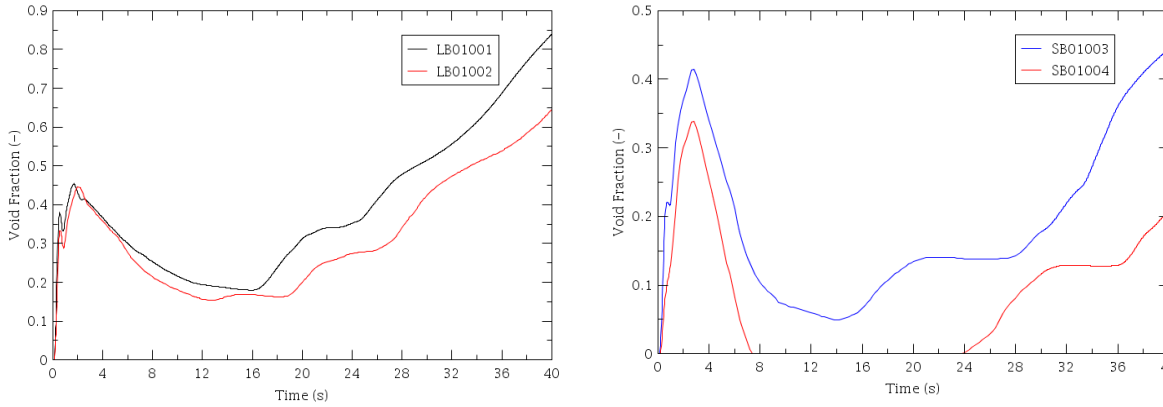

Fig. 8. Average void fraction calculated by RELAP5 on exit of active region in hot channel

It is clearly observed that the more break size larger the more amount of void fraction appears during given transient time. When the coupling of LOCA and SBO occurs, at the moment before 4 seconds, due to pressure drop, void fraction appears with the peak larger than 0.4 with LBLOCAs and equal or less than 0.4 with SBLOCAs. Then, due to reactor scram, heat source is decreased and void fraction is also reduced for a while. Later, pressure drop and decay heat cause void fraction increasing again as in Figure 8.

C. Sub channel code CTF analysis for void fraction

It is not practical to simulate the whole hot channel in CTF because of large channels in a bundle of fuel assembly. So a part as the twelfth ofthe assembly is taken to be representative for whole bundle for void fraction prediction with its power approximate of the twelfth of the whole bundle as illustrated in Figure 9.

The selected part in Figure 9 with relative power of 27.7 is well approximate to value 27.6, the twelfth of the whole bundle power. Figure 10 shows the CTF cross section modeling of the channels in the selected part. The initial and boundary data for CTF simulation are taken from MCNP5 and RELAP5 calculation results as following: (a) axial channel power distribution and relative power for each rod are taken from MCNP5 output, (b) pressure; mass flow rate, enthalpy and total power in transient of 40 s are taken from RELAP5 output. For each case, CTF runs for 30s to get steady state and then next 40s CTF runs in transient.

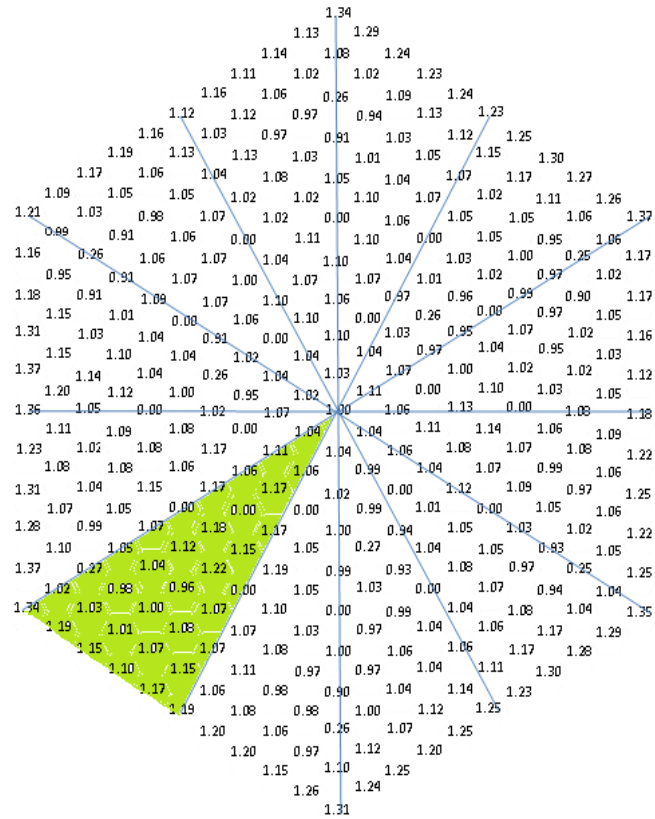

Fig. 9. the twelfth of whole bundle taken for representative for void fraction prediction.

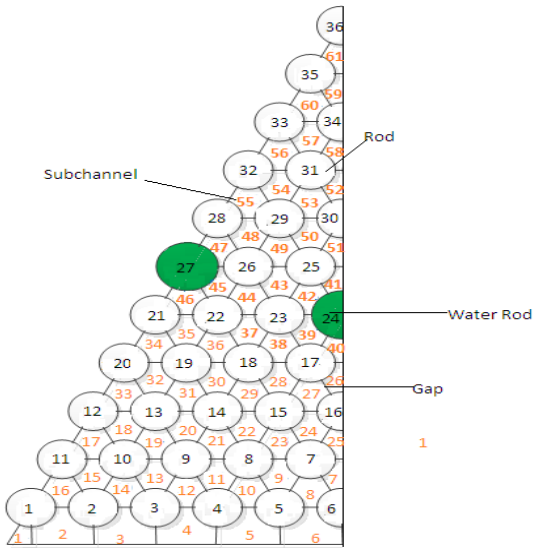

Fig. 10. the cross section of CTF modeling for the selected part of the whole bundle

For axial channel simulation, the number of vertical levels is 40 with different vertical divisions. The first section consists of 30 levels with vertical cell length 0.103 m while the top of active part consists of 10 levels with vertical cell length 0.044125 m. Therefore, the part in the graph (b) of Figure 7 is zoomed in with finer scale by CTF modeling with 10 vertical divisions and cross section as in Figure 10. Because CTF is considered as 3D modeling code, it is expected to get improved results in comparison with RELAP5. Figure 11 and 12 show the comparison of void fraction prediction by RELAP5 and CTF at three positions: inlet, middle and outlet of zooming part. It is observed that CTF prediction is always higher than RELAP5 in 4 cases.

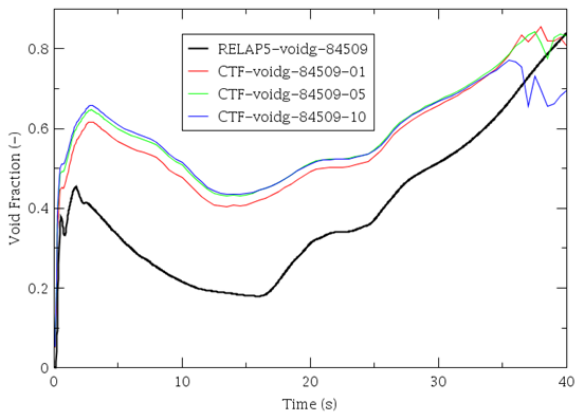

(LB01001)

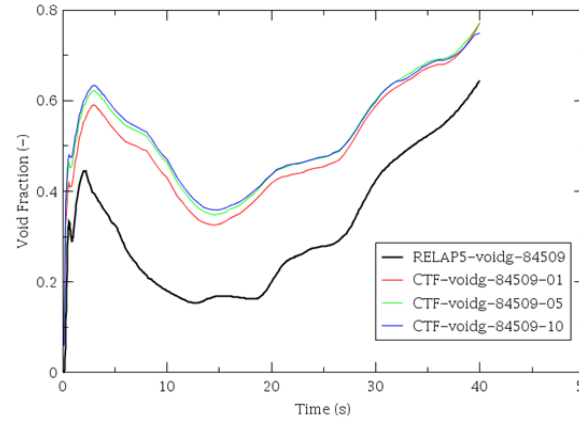

(LB01002)

Fig. 11. Void fraction prediction by CTF and RELAP5 for LBLOCAs

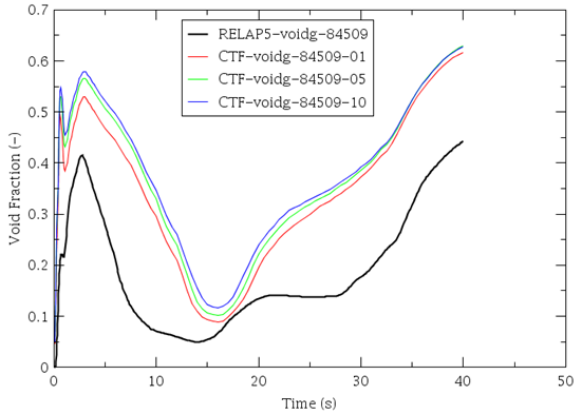

(SB01003)

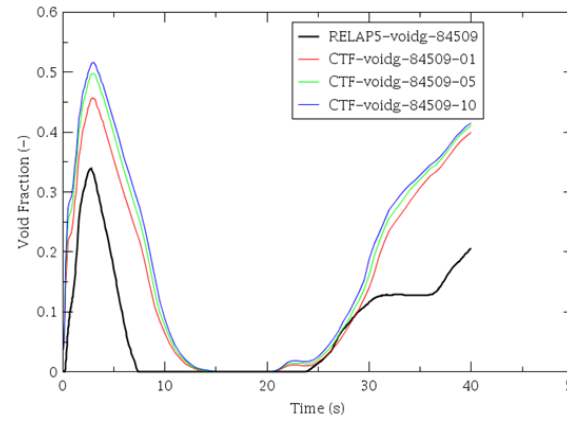

(SB01004)

Fig. 12. Void fraction prediction by CTF and RELAP5 for SBLOCAs

D. Discussion on RELAP5 and CTF void fraction predictions

Different treatment approach between RELAP5 and CTF

Regarding to the phase change of four cases studied in RELAP5 by formula (1), it is observed that, vapor generation happens at two situations: (a) phase change at interfacial area given by expression:$-\frac{H_{ig}(T^s-T_g)+H_{if}(T^s-T_f)}{(h_g^*-h_f^*)}$ and (b) phase change near wall denoted by Γ_w. The total vapor generation rate and evaporation rate near wall, Γ_w for LB01001, LB01002, SB01003 and SB01004 are presented in Figure 13 and Figure 14, respectively. It is shown that Γ_w in all cases is nearly equal to total vapor generation rate, so the void fraction predictions due to phase change at interfacial area for these casesare very small.

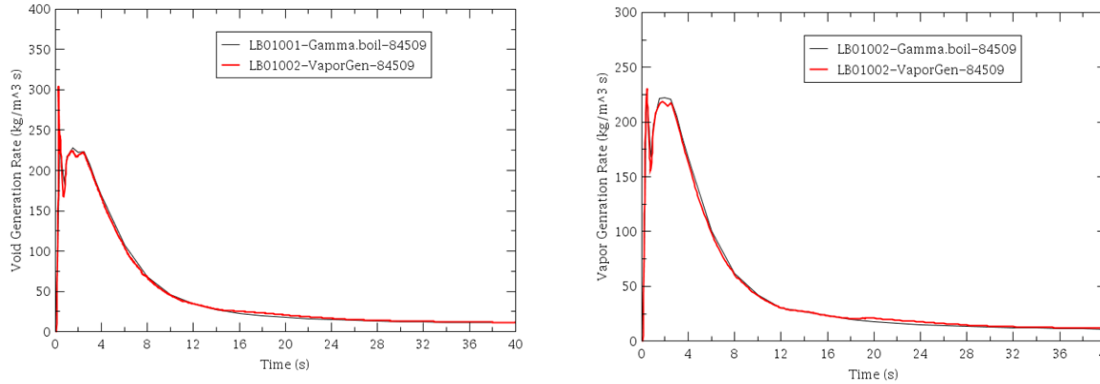

Fig. 13. Total vapor generation rate and vapor generation rate near wall for LB01001 and LB01002

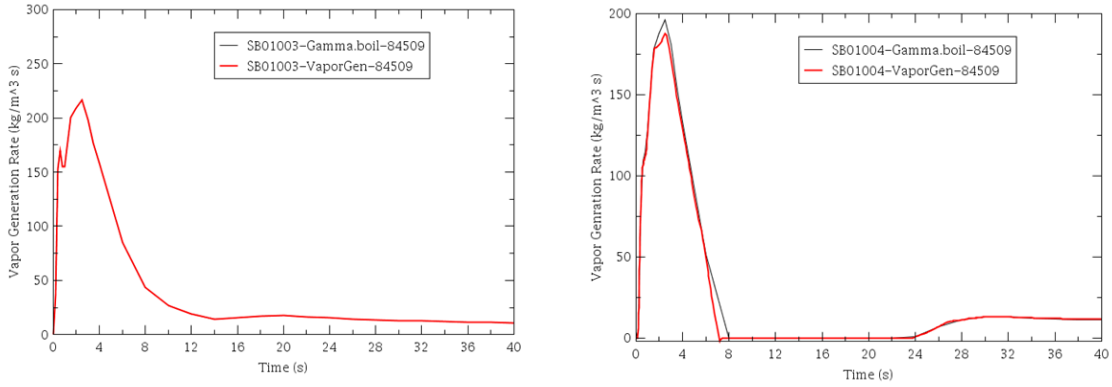

Fig. 14. Total vapor generation rate and vapor generation rate near wall for SB01003 and SB01004

For instant, with the case of LB01002, the data related to evaporation of interfacial area at the 15s of transient are given in Table 4. So the vapor generation rate of interfacial area, $-\frac{H_{ig}(T^s-T_g)+H_{if}(T^s-T_f)}{(h_g^*-h_f^*)}$ is calculated as 0.014240788 (kg/m3s) which is very small in comparison with total vapor generation rate at this moment,Γ_w as 25.181887 (kg/m3s).

Table IV. Data related to phase change of interfacial area for case LB01002B at 15s of transient

Pressure (bar)	Liquid Enthalpy (j/kg)	Evaporation Enthalpy (j/kg)	Vapor Enthalpy (j/kg)	Hif (*) (W/m3K)	Hig(*) (W/m3K)	Liquid temp (K)	Vapor temp (K)	Saturation temp (K)
82.19	1.33E+06	1.42E+06	2.75E+06	9.57E+05	1.06E+08	570.13	570.05	570.05

(*) these terms as in formula (1)

The correlation used to calculation of Γ_w is presented in [11]. Due to RELAP5 calculates just one liquid temperature in a volume and does not calculate thermal gradients in the wall boundary layer. So In this case, the bulk liquid can be subcooled while water in the boundary layer iswarmer and is flashing to steam as Lahey mechanistic method for nucleate, transition, and film boiling. As mentioned in [13], the prediction of the conditions necessary for existing net voids is calculated by Saha-Zuber method. Then Lahey's method of assigning a fraction of the total heat flux to liquid, which causes flashing at the wall, is applied.

$$\Gamma_w = \frac{q_f^{"} A_w}{V\left(max\left(h_g^s - h_f, 10^4 \frac{J}{kg}\right)\right)} Mul \qquad (9)$$

The detail of formula (9) is presented in [13].

For CTF void fraction prediction, the vapor generation rate is given as formula (6). In four cases studied the heat transfer belongs to mode of nucleate boiling or sub cooled boiling. Thus, for the normal wall model in CTF, liquid is assumed to cover all heated area and all heat from the wall is transfer to liquid. The vapor generation rate is caused from phase change due to increase of liquid enthalpy. The interfacial heat transfer coefficients are presented in [14] corresponding to flow regime. For instant, interfacial heat transfer coefficient for sub cooled, $h_{i,scl}$is defined flow with bubble and large bubble as following:

$$h_{i,scl} = \frac{1}{\sqrt{\pi}} \left(\frac{k_l U_{vl}}{r_b} \rho_l C_{pl}\right)^{1/2} \qquad (10)$$

Heat transfer coefficient from wall to liquid is also affected to phase change. It is observed that with four cases studied flow regimesare sub cooled boiling or nucleate boiling and Chen [11, 12] correlation are used in both of RELAP5 and CTF codes.Anyway, for RELAP5, heat from the wall is portioned into two parts:

$$Q_{wf} = Q_{conv} + Q_{boil} \qquad (11)$$

Whrere, the item Q_{boil} is causes near wall boiling term, Γ_w as mentioned above.

Accuracy of void faction predictions

- Geometry of flow in modeling

Due to RELAP5 model of flow is 1D, so that the flow through hot channel including 312 fuel rods is simulated as the flow in a pipe with equivalent flow area of 0.02538 m2 as mentioned in Table 28. The conversion of geometry of flow in RELAP5 causes inaccuracy in flow regime in comparison with origin flow. This issue affects to accuracy of void fraction. In other hand CTF model of flow is 3D as illustrated in Figure 49 with P equal 12.75 mm and D equal 9.1 mm. Therefore, the flow at scale of sub channel is modeled properly.

- Determine temperature of liquid near wall

For the RELAP5 model, the temperature is averaging inside a control volume. Therefore, the temperature of liquid near wall is the same at the center of the flow. For example, with the flow area of 0.02538 m2 then the distance from center of flow to the wall is around 9 cm. For the CTF model of flow is based on sub channel geometry as in Figure 49, and then the distance from the center of flow to the wall is about 0.275 cm.

It is concluded that the physical models for phase change of RELAP5 and CTF presented in formulas (6), (7) and (8), (16), respectively, is depended on near wall liquid enthalpy (or temperature). CTF gives the near wall enthalpy better than RELAP5, and then its calculation of phase change is more accuracy. Besides, the conversion of flow is not implemented as in RELAP5, so that, the flow regime in CTF model is reliable.

Based on above arguments and the fact that CTF can predict void fraction with pressure

of 3MPa and 7MPa with acceptable accuracy such as BM ENTEK tests [15], it is concluded that CTF gives better void fraction prediction results than RELAP5.

CONCLUSIONS

It is summarized some achievements from present study as following:

- Multi codes MCNP5, RELAP5, CTF are used to simulated system scale and bundle of channel scale of the VVER-1000/V392 reactor with initial data for RELAP5 and CTF calculated by MCNP5 code.
- The system and bundle of channel scales are used to analysis of void fraction predictions for hot channel of VER-1000/V392 reactor with higher prediction by CTF.
- The reason of different results of RELAP5 and CTF mainly come from different physical models to treat phase change at the interfacial area and near wall and also from partition of wall heat transferred to liquid. The item of near wall boiling, Γ_w in RELAP5 proposed by Laheymechanistic method may not give enough accuracy of void fraction prediction as smaller scale code as CTF.

ACKNOWLEDGMENT

The authors of this paper wish to express their appreciation for the financial support from Ministry of Science and Technology (MOST) through the National R&D Project: "Study the Nuclear Power Plant's Technology proposed for NinhThuan 1 and NinhThuan 2 in order to support Basic Design's Review", code KC.05.26/11-15. The authors of this paper also wish to express their appreciation to Mr. Duong Quoc Hung, Ph.D. for his exchange information of CTF training between Vietnam Agency for Radiation and Nuclear Safety (VARANS) and Pennsylvania State University (PSU).

NOMENCLATURE

$A'''_{int,scl}$	Sub-cooled liquid interfacial area per unit volume (m^1)	$\dot{m}_k^{TM}$	Mass exchange of phase k ($kg/m^2.s$)
$A'''_{int,scv}$	Sub-cooled vapor interfacial area per unit volume (m^1)	P_l	Density of liquid (kg/m^3)
$A'''_{int,shl}$	Super-heated liquid interfacial area per unit volume (m^{-1})	Q_{wf}	Wall heat transfer to liquid (W)
$A'''_{int,shv}$	Super-heated vapor interfacial area per unit volume (m^{-1})	Q_{conv}	Wall heat transfer to liquid for convection (W)
A_s	Conductor surface area in mesh cell (m^2)	Q^w_{if}, Q_{boil}	Wall heat transfer to liquid for vaporization (W)
A_x	Mesh-cell area, X normal (m^2)	T_g	Vapor temperature (K)
C_{pl}	Liquid specific heat, constant pressure (J/kg.K)	T^S	Saturated temperature (K)
C_{pv}	Vapor specific heat, constant pressure (J/kg.K)	T_{crit}	Critical heat flux temperature (K)
$\bar{G}$	Mixing mass flux ($kg/m^2.s$)	T_l, T_f	Liquid temperature (K)
$h_{g,sat}$	Vapor saturation enthalpy (J/kg)	r_b	Bubble diameter (m)
$h_{int,scl}$	Sub-cooled liquid interface heat transfer coefficient (W/m2.K)	α_{ki}	Void fraction of phase k induced by sub channel i
$h_{int,scv}$	Sub-cooled vapor interface heat transfer coefficient (W/m2.K)	α_{kiEQ}	Equilibrium quality void fraction
$h_{int,shl}$	Super-heated liquid interface heat transfer coefficient (W/m2.K)	β_{TP}	Two phase turbulent mixing coefficient
$h_{int,shv}$	Super-heated vapor interface heat transfer coefficient (W/m2.K)	ρ_{ki}	Density of phase k in sub channel i (kg/m^3)
h_c	Chen correlation heat transfer coefficient ($W/m^2.K$)	ρ_l	Liquid density (kg/m^3)
h_l^*	Liquid enthalpy (J/kg)	ρ_v	Vapor density (kg/m^3)
$h_{l,sat}$	Liquid saturation enthalpy (J/kg)	$\bar{\rho}, \rho_m$	Mixing density (kg/m^3)
h_g	Vapor enthalpy (J/kg)	Γ'''	Volumetric mass flow rate (kg/m3.s)
h_{if}	Vapor interface heat transfer coefficient ($W/m^3.K$)	Γ_w	Vapor generation from near wall (kg/m3.s)
h_{ig}	Liquid interface heat transfer coefficient ($W/m^3.K$)	Γ_g	Total Vapor Generation ($kg/m^3.s$)
$\dot{m}_k^{VD}$	Mass exchange due to drift model (kg/s)	ΔX	Mesh-cell axial height (m)

REFERENCES

[1]. Information Systems Laboratories, Inc., Rockville, Maryland, Idaho Falls, Idaho. "RELAP5/MOD3.3 Code Manual, Vol. II, Appendix A Input Requirements, pp. 12, 234", December 2001.

[2]. Dominique Bestion., "From the direct numerical simulation to system codes - perspective for the multi-scale analysis of LWR thermal hydraulics", Nuclear Engineering and Technology, Vol.42 No.4, pp.609-619, December 2010.

[3] VVER-1000 Coolant Transient Benchmark "PHASE 1 (V1000CT-1) Vol. I: Main Coolant Pump (MCP) switching On - Final Specifications", NEA/NSC/DOC (2002)6.

[4] S.K. Agrawal, Ashok Chauhan, Alok Mishra "The VVERs at KudanKulam", Nuclear Engineering and Design 236, 812–835, 2006.

[5] Division of Systems Research Office of Nuclear Regulatory Research U. S. Nuclear Regulatory Commission Washington, DC 20555 "RELAP5/MOD3.3 CODE MANUAL VOLUME I: CODE STRUCTURE, SYSTEM MODELS, AND SOLUTION METHODS", Information Systems Laboratories, Inc. Rockville, Maryland Idaho Falls, Idaho, pp. 20-34, December 2001.

[6] M. Avramova, A. Velazquez-Lozada, and A. Rubin., "Comparative Analysis of CTF and Trace Thermal-Hydraulic Codes Using OECD/NRC PSBT Benchmark Void Distribution Database", Hindawi Publishing Corporation, Science and Technology of Nuclear Installations, Volume 2013, Article ID 725687, pp. 2-5, Accepted 16 November 2012.

[7] Robert K. Salko., "Improvement of COBRA-TF for modeling of PWR cold- and hot-legs during reactor transients", A dissertation in Nuclear Engineering for the Degree of Doctor of Philosophy, The Pennsylvania State University, pp. 7-17, May 2012.

[8] Risk Engineering LTD, Sofia 1618, Bulgaria 10, Vihren Str. "Nuclear Power Technology Consideration, Project Science and Engineering Document" (Reference Number REL-885-SG-4.1), pp. 8-9, December 2012.

[9] Risk Engineering LTD, INTRODUCTION IN VVER TECHNOLOGIES. "Training course provided for Vietnam Atomic Energy Institute VINATOM", Sofia, Bulgaria, 15Jan – 9 March 2012.

[10] Hoang Minh Giang, Nguyen Phu Khanh, Le Van Hong., "Capability analysis of passive systems in typical design extension conditions for nuclear reactor VVER-1000/V392", Journal of Science and Technology 52 (2C), pp. 81-92, 2014.

[11] Risk Engineering LTD, Sofia 1618, Bulgaria 10, Vihren Str. "Nuclear Power Technology Consideration, Project Science and Engineering Document" (Reference Number REL-885-SG 6.9.3), pp. 9-29, December 2012.

[12] Risk Engineering LTD, Sofia 1618, Bulgaria 10, Vihren Str. "Nuclear Power Technology Consideration, Project Science and Engineering Document" (Reference Number REL-885-SG 4.2), pp. 17-18, December 2012.

[13]. Information Systems Laboratories, Inc., Rockville, Maryland, Idaho Falls, Idaho. "RELAP5/MOD3.3 Code Manual, VOLUME IV: MODELS AND CORRELATIONS", pp. 209-212, 108-111, December 2001.

[14] M. J. Thurgood, J. M. Kelly, T. E. Guidotti, R. J. Kohrt, K. R. Crowell., "COBRA/TRAC - A Thermal-Hydraulics Code for Transient Analysis of Nuclear Reactor Vessels and Primary Coolant Systems, Equations and Constitutive Models", NUREG/CR-3046, PNL-4385, Vol. 1, pp. 3.15-3.22, 4.16-4.18, March 1983.

[15] Hoang Minh Giang, Hoang Tan Hung, Nguyen PhuKhanh, "Investigation of CTF void fraction prediction by ENTEK BM experiment data", acceptance to be published in Nuclear Science and Technology (ISSN 1810-5408), 2015.

[16] VVER-1000 MOX core Computational Benchmark, Specification and Results, Expert Group on Reactor - based Plutonium Disposition, Eugeny Gomin, Mikhail Kalugin, Dmitry Oleynik Russian Research Centre, Kurchatov Institute, NEA No 6088, © OECD 2006.